

In-situ shifted excitation Raman difference spectroscopy: development and demonstration of a portable sensor system at 785 nm

M. Maiwald, A. Müller, B. Sumpf
Ferdinand-Braun-Institut, Leibniz-Institut für Höchstfrequenztechnik,
Gustav-Kirchhoff-Str. 4, 12489 Berlin, Germany

ABSTRACT

In-situ shifted excitation Raman difference spectroscopy (SERDS) experiments are presented using a portable sensor system. Key elements of this system are an in-house developed handheld probe with an implemented dual-wavelength diode laser at 785 nm. An optical power of 120 mW is achieved ex probe. Raman experiments are carried out in the laboratory for qualification using polystyrene as test sample. Here, a shot-noise limited signal-to-noise ratio (SNR) of 120 is achieved. Stability tests were performed and show a stable position of the Raman line under study within 0.1 cm^{-1} and a stable Raman intensity better $\pm 2\%$ mainly limited by shot noise interference. SERDS experiments are carried out in an apple orchard for demonstration. Green apple leaves are used as test samples. The Raman spectra show huge background interferences by fluorescence and ambient daylight which almost obscure Raman signals from green leaves. The selected excitation power is 50 mW and the exposure time is 0.2 s to avoid detector saturation. SERDS efficiently separates the Raman signals from fluorescence and daylight contributions and generates an 11-fold improvement of the signal-to-background noise with respect to the measured Raman signals. The results demonstrate the capability of the portable SERDS system and enable rapid in-situ and undisturbed Raman investigations under daylight conditions.

Keywords: Raman spectroscopy, Shifted excitation Raman difference spectroscopy, SERDS, 785 nm, diode laser

1. INTRODUCTION

Raman spectroscopy is a powerful analytical tool and besides many fundamental research fields this spectroscopic technique has been demonstrated in several so-called real-world applications such as point-of-care diagnostic¹, food inspection², and geological investigations³. The development of wavelength stabilized diode lasers as excitation light sources, fiber coupled probes, and miniaturized CCD based spectrometers enable the realization of portable sensors such as handheld devices suitable for in-situ investigations. For Raman spectroscopy the laser line at 785 nm is one of the most popular wavelengths. Here, the excitation in the NIR spectral range has the potential to generate less fluorescence especially for investigating biological samples. Beside this, Si-based CCD multichannel detectors are still sensitive enough and can be used to detect Stokes-shifted Raman signals in the “fingerprint” spectral range. However, the weak Raman signals could still be covered by fluorescence. Moreover, in-situ measurements have to overcome ambient light such as daylight interferences. Both background signals can cause detector saturation even at exposure times of a few seconds or even below one second for a single Raman spectrum.

Shifted excitation Raman difference spectroscopy (SERDS) and related techniques have been demonstrated as a powerful spectroscopic tool to separate Raman signals from background interferences⁴⁻¹⁰. In contrast to related methods, for SERDS only two Raman spectra excited with two slightly shifted laser wavelengths are necessary and the method has the potential to reduce the overall measurement time. The latter is preferred to achieve rapid on-site decisions directly after the measurement, e.g., for in-vivo cancer diagnosis during medical surgery and the detection of explosives at airport security checks. The spectral distance of the two emission wavelengths should be close to the bandwidth of the Raman lines under study⁶. Raman lines of condensed samples show typical line widths of $3\text{-}12 \text{ cm}^{-1}$ (FWHM)¹¹.

*Martin.Maiwald@FBH-Berlin.de; phone +49.306392-2651; fax+49.306392-2642; www.fbh-berlin.de

A monolithic diode laser based excitation light source without movable parts together with low power consumption is preferred to realize a compact and robust portable and battery driven SERDS sensor system. Monolithic dual-wavelength diode lasers with an emission at 785 nm suitable for Raman spectroscopy and SERDS were presented by our group recently^{12,13}. Moreover, we developed and fabricated a compact handheld Raman probe. Here, a dual-wavelength diode laser at 785 nm similar to the above mentioned device was implemented and Raman experiments were carried out for qualification¹⁴.

In this paper we present a portable SERDS system using the above mentioned handheld Raman probe and outdoor SERDS experiments are performed for demonstration. First, the diode laser module at 785 nm and the handheld SERDS probe is described and Raman experiments performed in the laboratory for qualification are presented. After this, the portable SERDS system is shown and outdoor SERDS experiments in the apple orchard using green apple leaves measured directly on the tree are presented. The results demonstrate that the portable sensors system is suitable for in-situ SERDS experiments. This enables rapid and undisturbed outdoor Raman investigations and provides on-site decisions immediately after the measurement.

2. RAMAN PROBE WITH AN INTEGRATED DUAL-WAVELENGTH DIODE LASER

2.1 Description of the diode laser module

Figure 1 shows a scheme of the diode laser module. The core element of the module is a dual-wavelength diode laser emitting at 785 nm. The single chip has a size of 3.0 mm x 0.5 mm. The device is fabricated using metal organic vapor phase epitaxy (MOVPE) and consists of two laser resonators. At the rear side of each cavity a 10th order distributed Bragg reflector (DBR) grating is implemented and the gratings have a spatial distance of 80 μm. These wavelength selective elements provide two excitation lines at 785 nm with a spectral spacing of about 10 cm⁻¹ for SERDS. Ridge waveguides (RW) are fabricated with a stripe width of 2.2 μm to guide the laser light. A Y-branch coupler is used to couple the laser light of both resonators into a common RW section to realize a common output aperture and thus one excitation spot at the sample for both excitation wavelengths. The rear facet is anti-reflective coated with $R_r \leq 10^{-3}$. The front facet of the semiconductor chip has a reflectivity of $R_f = 5\%$ and acts as the second laser resonator mirror. Separate electrical contacts are realized which are indicated with C₁, C₂, C_Y, and C_{out} and allow an individual control of each excitation wavelength for SERDS. A detailed description of the dual-wavelength diode laser and Raman experiments which demonstrate the suitability of the device for SERDS is given in Ref. ^{12,13}.

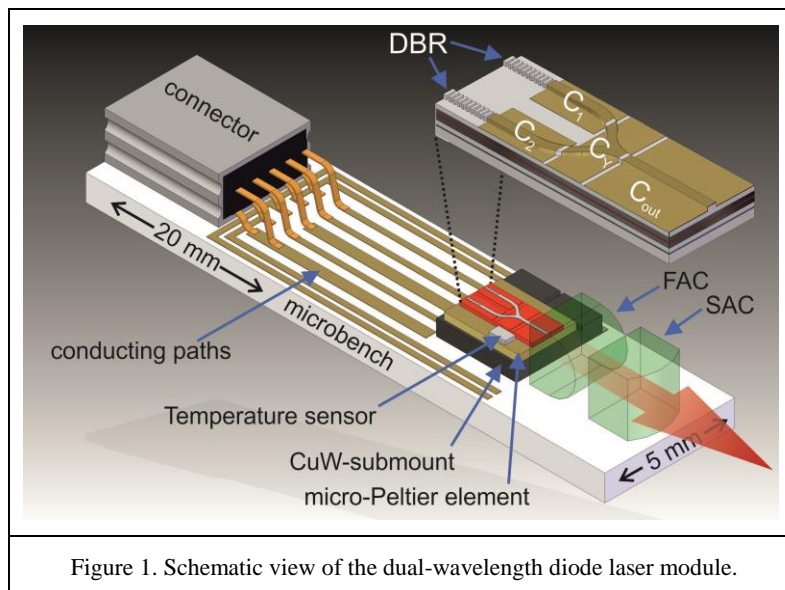


Figure 1. Schematic view of the dual-wavelength diode laser module.

The dual-wavelength diode laser is soldered p-side up on a copper tungsten (CuW) heat spreader using Au/Sn. This sub-assembly is mounted on a micro-Peltier element (eTEC™ HV56, Laird Technologies Gothenburg AB) on an AlN-microbench for heat transfer. The microbench has a footprint of 20 mm x 5 mm and acts as a baseplate for the laser

module. Conducting paths on the AlN-microbench and a micro connector are used as electrical contacts for the diode laser, a temperature sensor, and the micro-Peltier element.

Based on the optical properties of the diode laser and optical simulations a fast axis collimator lens (FAC) with a focal length of $f_{FAC} = 700 \mu\text{m}$ and a slow axis collimator lens (SAC) with $f_{SAC} = 1500 \mu\text{m}$ are mounted on the microbench to collimate the laser beam.

2.2 Description of the SERDS probe

The above described dual-wavelength diode laser module is integrated in an in-house developed SERDS probe as the excitation source. A schematic inside view is presented in Fig. 2. Here, the collimated laser light passes a laser bandpass filter (MaxLine® laser clean-up filter, Semrock) to suppress residual amplified spontaneous emission. Two 785 nm long-pass edge filter (RazorEdge®, Semrock) are positioned at 5° to the incident beam. These filters are highly reflecting at 785 nm and direct the excitation beam to the probe head.

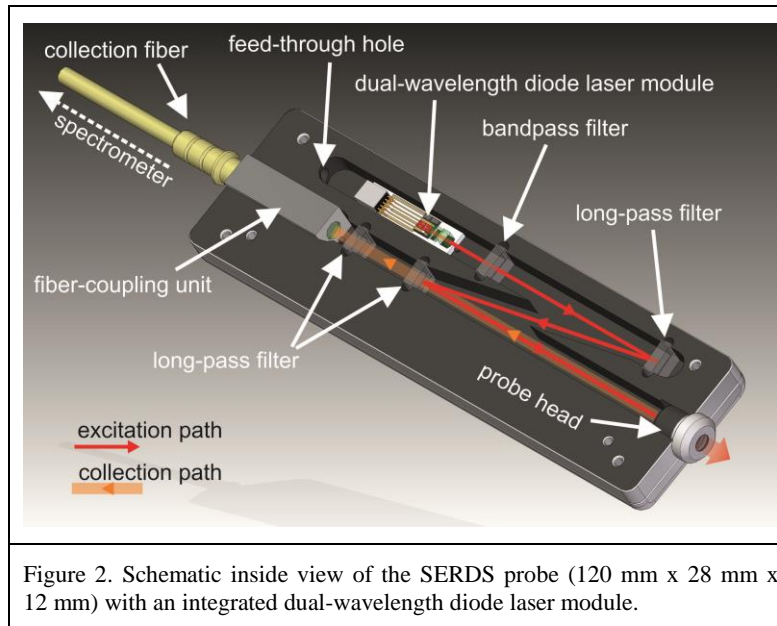


Figure 2. Schematic inside view of the SERDS probe (120 mm x 28 mm x 12 mm) with an integrated dual-wavelength diode laser module.

This probe head contains a customized aspheric lens. Based on optical simulations this lens was designed with a focal length of 2.4 mm and a numerical aperture of $NA = 0.8$, which allows to realize a compact handheld probe and to achieve high collection efficiency for inelastic scattered light. A 0.5 mm thick quartz glass window protects the inner parts of the SERDS probe.

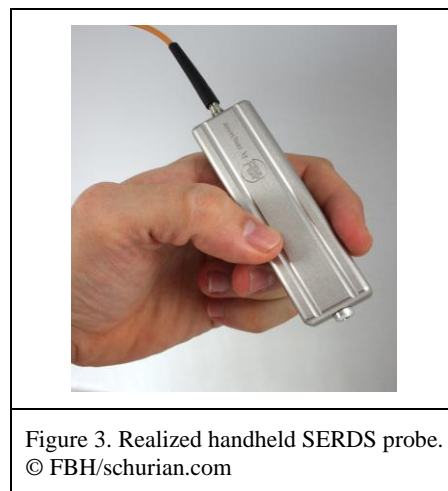


Figure 3. Realized handheld SERDS probe.
© FBH/schurian.com

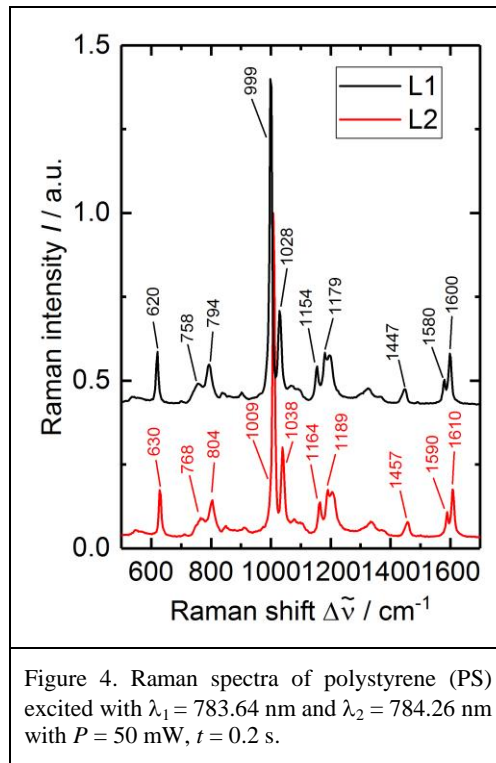
The 180°-backscattered light is collected by the customized aspheric lens and is directed to two long-pass edge filters. Here, the laser light, the elastic scattered light, and the anti-Stokes shifted light is highly reflected. The Stokes shifted light passes both filters and a fiber-coupling unit which contains an achromatic lens with a focal length of 10 mm (Thorlabs GmbH) couples the Raman photons into a multimode fiber ($d_{\text{core}} = 105 \mu\text{m}$, $\text{NA} = 0.22$). The probe housing has a dimension of 100 mm x 28 mm x 12 mm and is milled from aluminum. The inner surface is coated black (Magic Black™, Acktar Ltd.) in order to avoid stray light interference. A realized handheld SERDS probe is presented in Fig. 3.

The collection fiber is connected to a compact spectrograph (HyperFlux U1, Tornado Spectral Systems). This spectrometer has a spectral resolution of 8 cm^{-1} and the spectral dispersed light is focused onto a CCD (MityCCD-H10141, 2048 x 512 pixel). Here, the operating temperature is -10°C .

Before the outdoor experiments Raman measurements were performed to qualify the SERDS probe.

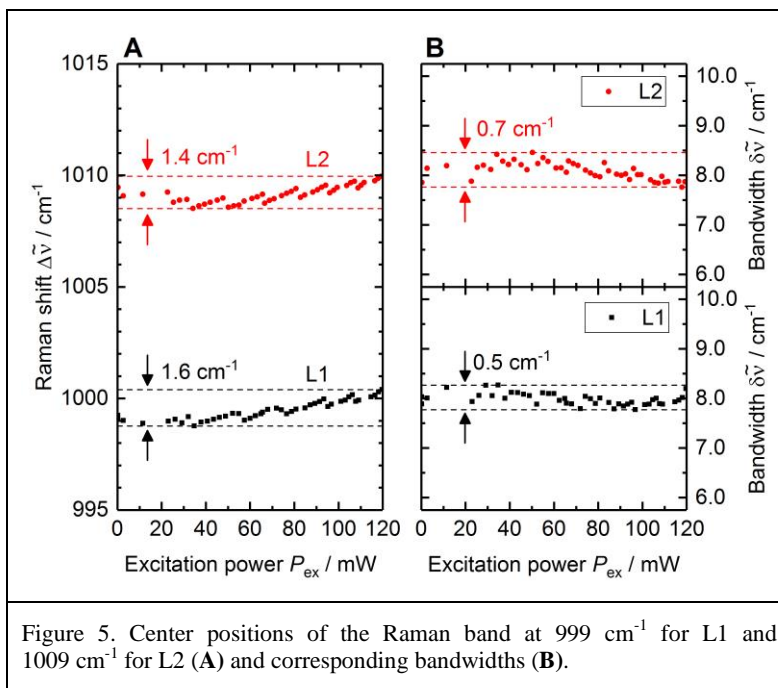
2.3 Performance of the handheld SERDS probe

Raman spectra of polystyrene (PS) were measured with the SERDS probe for qualification and are presented in Fig. 4. The spectra L1 and L2 were generated using excitation lines at 783.64 nm and 784.26 nm, respectively. For both excitations the optical power at sample was 50 mW. This was realized using the injection currents for the diode laser with $I_{C1} = 90 \text{ mA}$ for L1 and $I_{C2} = 95 \text{ mA}$ for L2. Here, and for all further experiments the current at C_Y and C_{out} is constant with $I_{C_{\text{out}}} = 35 \text{ mA}$ and $I_{C_Y} = 0 \text{ mA}$. The temperature at the diode laser module is 25°C . The spectra show one accumulation with 0.2 s exposure time. The intensity of each spectrum is normalized to 1 and L1 has an offset for clarity. Within the investigated fingerprint spectral region all Raman lines of PS are clearly visible and resolved. The positions of the Raman bands of L1 are used for wavelength calibration according to literature values¹⁵. The positions of L2 are shifted by 10 cm^{-1} , as expected.

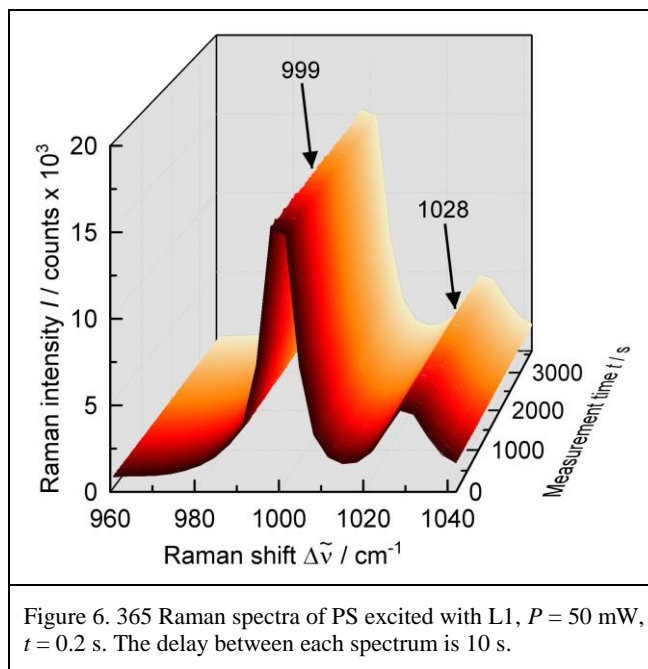


By changing the injection currents I_{C1} and I_{C2} from 0 mA to 400 mA the excitation power at sample can be adjusted from 0 mW to 120 mW with respect to the analyte under study. Figure 5 A shows the center position of the Raman band of PS at 999 cm^{-1} for L1 and 1009 cm^{-1} for L2 versus the excitation power. For each laser line the optical power was adjusted from 0 mW to 120 mW by the corresponding injection current with a step size of 5 mA. The center positions for L1 and L2 are within a spectral window smaller than 2 cm^{-1} over the whole operating range and show a mean spectral distance between both Raman lines of $(9.7 \pm 0.5) \text{ cm}^{-1}$. Spectral shifts of the center positions to lower wavenumbers occurs with

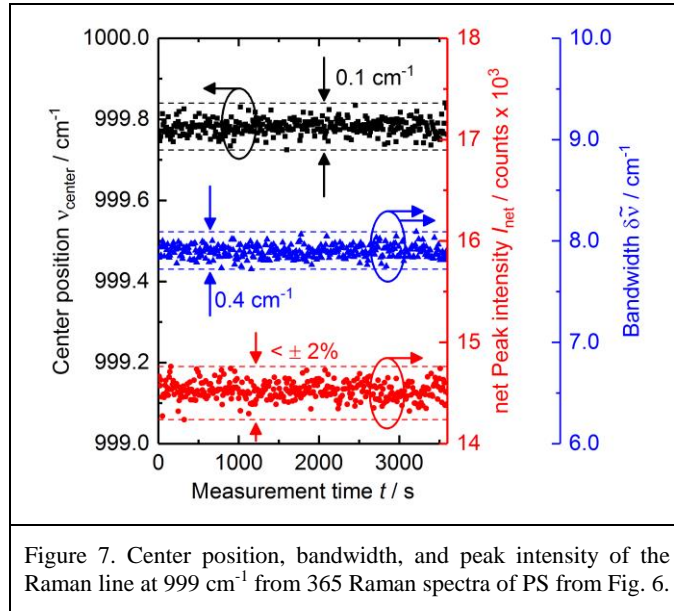
0.37 cm^{-1} corresponding to mode hops of the emission wavelengths of the light source typical for DBR diode lasers. Additionally, in Fig. 5 B the corresponding bandwidths (FWHM) of the Raman line for L1 and L2 are presented. Both Raman signals show a stable band width around 8 cm^{-1} and variations smaller than 1 cm^{-1} over the whole excitation power range. The shifts of the center position and the variations of the band width are within the pixel resolution of 3 cm^{-1} of the used spectrometer and the results enable a flexible choice in excitation power during Raman investigations without the necessity of a spectral recalibration of the spectrometer.



Stability tests were performed. Here, 365 successive Raman spectra of PS were measured with L1, $P_{\text{ex}} = 50 \text{ mW}$, and one accumulation with 0.2 s integration time.



Between each spectrum a delay of 10 s is used which leads to a total measurement time of about 1 hour. A temperature difference of 11 K between the laser module with 25°C and the probe housing with 36°C was realized using a heat plate simulate handheld operating condition. All 365 Raman spectra of PS between 960 cm^{-1} and 1040 cm^{-1} are presented in Fig. 6. The Raman lines show nearly identical signal distribution in the spectral region under study. No significant change in the shape of the Raman lines and variations in intensity is observed.



A more detailed analysis of the position of the Raman line at 999 cm^{-1} , the bandwidth, and the peak intensity versus the measurement time is given in Fig. 7. Here, the center position of the Raman band under study is within a spectral window of 0.1 cm^{-1} over the whole measurement time. Moreover, the bandwidth shows a peak-to-peak variation of $\pm 0.2 \text{ cm}^{-1}$. Both values are well below the pixel resolution of 3 cm^{-1} of the spectrometer. During these investigations the net peak intensity I_{net} of the Raman line at 999 cm^{-1} is about 14.500 counts and shows a peak-to-peak variation of $< \pm 2\%$ and a standard deviation $\sigma_{\text{peak-intensity}} \approx 90$ counts. As a result, using $\bar{I}_{\text{net}}/\sigma_{\text{peak-intensity}}$ a signal-to-noise ratio (SNR) of about 117 is calculated. This is close to the maximum reachable SNR within this measurement with $\text{SNR} = \sqrt{I_{\text{net}}} = 120$. Consequently, the intensity variations are mainly caused by shot noise interference.

The above presented results show the suitability of the developed handheld probe for Raman and SERDS spectroscopic investigation. A more detailed description of the laser module, the SERDS probe and the experiments concerning the qualification of the probe is given in Ref. 14.

3. OUTDOOR SERDS MEASUREMENTS FOR DEMONSTRATIONS

A handheld SERDS probe similar to the above described probe was applied in outdoor experiments to demonstrate the suitability of the device in a measurement scenario with laser induced fluorescence and daylight as background interference. In advance, the handheld probe was connected to a field operable measurement system. Here, the above used compact spectrometer is used for detection. The integrated dual-wavelength diode laser module from Fig. 1 is connected to four current sources (LDD 400, $I_{\text{max}} = 400 \text{ mA}$, Wavelength Electronics, Inc.) and one temperature controller (HTC1500, $I_{\text{max}} = \pm 1.5 \text{ A}$, Wavelength Electronics, Inc.). A USB Analog Output Module (RedLab 3103) is integrated into the system for communication. All elements including a 12 V battery which provides 25 Ah are arranged in a protector case (W+S Water Safety Europe GmbH). A laptop (Toughbook CF-53, Panasonic) and in-house developed software are used for data handling and control.

The developed portable SERDS system was used for in-situ measurements in the orchard during harvesting time at the beginning of September 2015 in Prangins, Switzerland and the realized device is presented in Fig. 8. Raman spectra of green apple leaves were measured for demonstration. These test samples were investigated in-situ and directly on the tree. For all Raman experiments the samples were excited with $L1 = 783.63 \text{ nm}$ and $L2 = 784.26 \text{ nm}$ and $P_{\text{ex}} = 50 \text{ mW}$.



Figure 8. Portable SERDS system used for outdoor experiments in the apple orchard.

Raman spectra of a green apple leaf are presented in Fig. 9 A as an example. Each spectrum shows a single accumulation with 0.2 s integration time. The Raman spectrum excited with L2 has an offset of 2,000 counts for clarity. Huge background intensity is observed in both spectra. Here, the intensity around 400 cm^{-1} is at the saturation level of the CCD detector with 65,535 counts. Additionally, an absorption spectrum of water vapor was simulated with a spectral resolution of 8 cm^{-1} comparable to the spectral resolution in our Raman measurements. The simulated spectrum is shown together with both measured Raman spectra in Fig. 9 A. The spectrum was calculated using the rotational-vibrational absorption lines as given in the HITRAN database¹⁶ in the spectral region under investigation. The simulated intensity distribution is comparable to the pattern of the background signal of both Raman spectra in the spectral range under study. Moreover, three additional dips in the Raman spectra are observed and are indicated with arrows. The positions of these dips presented in relative wavenumbers 988 cm^{-1} , 1049 cm^{-1} , and 1211 cm^{-1} corresponds to absolute wavenumbers 11541 cm^{-1} , 11704 cm^{-1} , and 11764 cm^{-1} and are identified as Fraunhofer lines of singly-ionized calcium (Ca II)¹⁷. Consequently, the background interference in the Raman spectra is mainly due to ambient daylight and contains signals from water vapor absorption from the atmosphere and intense Fraunhofer lines in the spectral region under study. Additionally, a residual laser induced fluorescence signal from the sample can be stated. Only a Raman line at 1526 cm^{-1} with a signal-to-background noise of $S/\sigma_B = 14$, is visible.

After the measurement, both Raman spectra from Fig. 9 A were subtracted and the shifted excitation Raman difference spectrum is presented in Fig. 9 B. Here, Raman signals are clearly separated from both background interferences, discussed above. An advanced in-house developed reconstruction algorithm¹⁸ was used to obtain a Raman spectrum in a conventional format. This algorithm includes a baseline correction and an integration of the signal distribution from Fig. 9 B. The so called reconstructed SERDS spectrum is presented in Fig. 9 C (1 x 0.2 s).

The reconstructed SERDS spectrum shows Raman lines of chlorophyll and carotenoids clearly resolved in the spectral region under study. The positions are indicated by dashed lines according to literature values¹⁹ and the signal-to-background noise of 160 for the Raman line at 1526 cm^{-1} , corresponding to an 11-fold improvement. Additionally, an average of ten Raman spectra of the investigated green leaf with 0.2 s integration time for each excitation line is measured at the same sample position and processed for SERDS. The corresponding reconstructed SERDS spectrum is presented in Fig. 9 C with an offset for clarity (10 x 0.2 s). Both reconstructed SERDS spectra show similar signal distributions and indicate reliable measurements and data processing. Further experiments on apples were performed and are described in detail in Ref. 20.

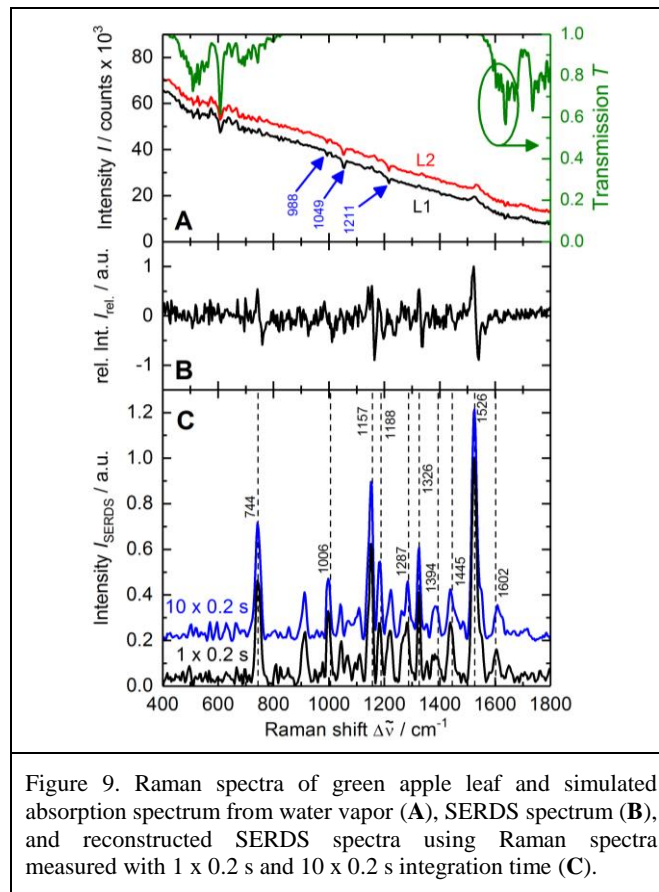


Figure 9. Raman spectra of green apple leaf and simulated absorption spectrum from water vapor (A), SERDS spectrum (B), and reconstructed SERDS spectra using Raman spectra measured with 1 x 0.2 s and 10 x 0.2 s integration time (C).

4. SUMMARY

In this contribution in-situ shifted excitation Raman difference spectroscopy (SERDS) experiments using a developed portable sensor system are presented. An in-house developed handheld SERDS probe with an implemented dual-wavelength diode laser at 785 nm was fabricated. The device provides a flexible excitation power up to 120 mW ex probe for both laser wavelengths for SERDS. Raman experiments were performed in the laboratory for qualification. Here, a shot-noise limited signal-to-noise ratio with 120 was achieved. Stability tests show a stable position of the Raman line under study within 0.1 cm^{-1} and a stable Raman intensity better $\pm 2\%$ mainly limited by shot noise interference. In-situ SERDS experiments in an apple orchard using green apple leaves were carried out for demonstration. The measured Raman spectra show huge background interferences by fluorescence and ambient daylight. The excitation power is 50 mW and the exposure time was 0.2 s in order to avoid detector saturation. SERDS efficiently separates the Raman signals from fluorescence and daylight contributions and generates an 11-fold improvement of the signal-to-background noise with respect to the measured Raman signals. The results demonstrate the capability of the portable SERDS system for outdoor experiments. This enables rapid and undisturbed in-situ Raman investigations and provides on-site decisions immediately after the measurement.

5. ACKNOWLEDGEMENT

The authors gratefully acknowledge Thomas Filler and Kamil Czajkowski from the prototype engineering group, Bastian Deutscher and Detlef Grimpe for technical assistance as well as Maria Krichler for software development. Parts of this work were realized within the projects DiLaRa (Zwei-Wellenlängen Diodenlasersystem für die Raman-Spektroskopie) and USER-PA (USability of Environmentally sound and Reliable techniques in Precision Agriculture). The authors gratefully acknowledge the financial support by the Federal Ministry of Education and Research (BMBF) in the program Validierung des Innovationspotenzials wissenschaftlicher Forschung – VIP under contract 03V0207 and the Federal office for Agriculture and Food under contract FKZ 2812ERA039, respectively.

REFERENCES

- [1] Matousek, P. and Stone, N., "Recent advances in the development of Raman spectroscopy for deep non-invasive medical diagnosis," *J. Biophotonics*, 6(1), 7-19 (2013).
- [2] Schmidt, H., Sowoidnich, K. and Kronfeldt, H.-D., "A Prototype Hand-Held Raman Sensor for the in-situ Characterization of Meat Quality," *Appl. Spectrosc.*, 64(8), 888-894 (2010).
- [3] Short, L., Thoms, A.V., Cao, B., Sinyukov, A. M., Joshi, A., Scully, R., Sanders, V., and Voronine, D. V., "Facile residue analysis of recent and prehistoric cook stones using handheld Raman spectrometry," *J. Raman Spectrosc.*, 46(1), 126-132 (2015).
- [4] Matousek, P., Towrie, M., Stanley, A., and Parker, A. W., "Efficient Rejection of Fluorescence from Raman Spectra Using Picosecond Kerr Gating," *Appl. Spectrosc.*, 53(12), 1485-1489 (1999).
- [5] Mosier-Boss, P. A., Liebermann, S. H., and Newberry, R., "Fluorescence Rejection in Raman Spectroscopy by Shifted-Spectra, Edge Detection, and FFT Filtering Techniques," *Appl. Spectrosc.*, 49(5), 630-638 (1995).
- [6] Zhao, J., Carrabba, M. M., and Allen, F. S., "Automated Fluorescence Rejection Using Shifted Excitation Raman Difference Spectroscopy," *Appl. Spectrosc.*, 56(7), 834-845 (2002).
- [7] Shreve, A. P., Cherepy, N. J., and Mathies, R. A., "Effective Rejection of Fluorescence Interference in Raman Spectroscopy Using Shifted Excitation Difference Technique," *Appl. Spectrosc.*, 46(4), 707-711 (1992).
- [8] McCain, S. T., Willett, R. M., and Brady, D. J., "Multi-excitation Raman spectroscopy technique for fluorescence rejection," *Opt. Exp.*, 16(15), 10975-10991 (2008).
- [9] Cooper, J. B., Abdelkader, M., and Wise, K. L., "Sequentially Shifted Excitation Raman Spectroscopy: Novel Algorithm and Instrumentation for Fluorescence-Free Raman Spectroscopy in Spectral Space," *Appl. Spectrosc.*, 67(8), 973-984 (2013).
- [10] Cooper, J. B., Marshall, S., Jones, R., Abdelkader, M., and Wise, K. L., "Spatially compressed dual-wavelength excitation Raman spectrometer," *Appl. Opt.*, 53(15), 3333-3340 (2014).
- [11] McCreery, R. L., [Raman spectroscopy for chemical analysis], John Wiley & Sons, Inc, New York, 73-94 (2000).
- [12] Maiwald, M., Eppich, B., Fricke, J., Ginolas, A., Bugge, F., Sumpf, B., Erbert, G., and Tränkle, G., "Dual-Wavelength Y-Branch Distributed Bragg Reflector Diode Laser at 785 Nanometers for Shifted Excitation Raman Difference Spectroscopy," *Appl. Spectrosc.*, 68(8), 838-843 (2014).
- [13] Sumpf, B., Maiwald, M., Müller, A., Fricke, J., Ressel, P., Bugge, F., Erbert, G., and Tränkle, G., "Comparison of two concepts for dual-wavelength DBR ridge waveguide diode lasers at 785 nm suitable for shifted excitation Raman difference spectroscopy," *Appl. Phys. B*, 120(2), 261-269 (2015).
- [14] Maiwald, M., Eppich, B., Ginolas, A., Sumpf, B., Erbert, G., and Tränkle, G., "Compact Handheld Probe for Shifted Excitation Raman Difference Spectroscopy with Implemented Dual-Wavelength Diode Laser at 785 Nanometers," *Appl. Spectrosc.*, 69(10), 1144-1151 (2015).
- [15] Schrader, B., [Raman-, Infrared atlas of organic compounds], Wiley-CVH, Weinheim, N-03 (1989).
- [16] Rothman, L. S., Gordon, I. E., Babikov, Y., Barbe, A., Chris Benner, D., Bernath, P. F., Birk, M., Bizzocch, L., Boudon, V., Brown, L. R., Campargue, A., Chance, K., Cohen, E. A., Coudert, L. H., Devi, V. M., Drouin, B. J., Fayt, A., Flaud, J.-M., Gamache, R. R., Harrison, J. J., Hartmann, J.-M., Hill, C., Hodges, J. T., Jacquemart, D., Jolly, A., Lamouroux, J., LeRoy, R. J., Li, G., Long, D. A., Lyulin, O. M., Mackie, C. J., Massie, S. T., Mikhailenko, S., Müller, H. S. P., Naumenko, O. V., Nikitin, A. V., Orphal, J., Perevalov, V., Perrin, A., Polovtseva, E. R., Richard, C., Smith, M. A. H., Starikova, E., Sung, K., Tashkun, S., Tennyson, J., Toon, G. C., Tyuterev, V. I., and Wagner, G., "The HITRAN2012 molecular spectroscopic database," *J. Quant. Spectrosc. Radiat. Transfer*, 130, 4-50 (2013).
- [17] Edlén, B., and Risberg, P., "The Spectrum of Singly-Ionized Calcium, Ca II," *Ark. Fys.* 10(6), 553-566 (1956).
- [18] Schmidt, H., Pérez Kaiser, D., and Maiwald, M., "International Patent, WO 2011/033017 A1" (2011).
- [19] Schrader, B., Klump, H. H., Schenzel, K., and Schulz, H., "Non-destructive NIR FT Raman analysis of plants," *J. Mol. Struct.*, 509(1-3), 201-212 (1999).
- [20] Maiwald, M., Müller, A., Sumpf, B., and Tränkle, G., "A portable shifted excitation Raman difference spectroscopy system: device and field demonstration," *J. Raman Spectrosc.* 47(10), 1180-1184 (2016).